

RESEARCH

Open Access



# Production of low wear friction lining material from agro-industrial wastes

Chinedum Ogonna Mgbemena<sup>1\*</sup> , Richard U. Esigie<sup>1</sup>, Chika Edith Mgbemena<sup>2</sup> and Chike M. Ata<sup>2</sup>

\*Correspondence:  
mgbemena.ogonna@fupre.  
edu.ng

<sup>1</sup>Department of Mechanical  
Engineering, Federal University  
of Petroleum Resources, Effurun,  
Nigeria

<sup>2</sup>Department of Industrial/  
Production Engineering, Nnamdi  
Azikiwe University, Awka, Nigeria

## Abstract

This research aims at producing and characterizing a low-wear friction lining material using a hybrid mixture of burnt vehicle tyres, pulverized palm kernel shell (PKS), pulverized coconut shell (CS), iron and brass filings obtained from the machine shop floor. The Taguchi method was used to determine the optimum parameter settings to obtain a friction lining with a low wear rate by exploring the signal-to-noise ratios (S/N) of the smaller-the-better. The developed friction lining was subjected to the scanning electron microscopy-energy dispersive spectroscopy (SEM-EDX) and X-ray fluorescence (XRF) to ascertain the functional groups present in the friction lining, their elemental composition and finally the morphology. The control factors used in the Taguchi analysis are the moulding temperature, cure time and heat treatment. The optimum parameter settings for a low wear rate were obtained as follows: moulding temperature of 175 °C, cure time of 8 min and heat treatment time of 3 h. The XRF spectroscopy indicated that the developed friction lining materials contained the following compounds in large proportions: CaO, SiO<sub>2</sub>, Al<sub>2</sub>O<sub>3</sub> and Fe<sub>2</sub>O<sub>3</sub>. The SEM-EDX results for the two image scans reported show that carbon and oxygen were the predominant elements observed in the micrograph.

**Keywords:** Automobile, Brakes, Brake pads, Characterization, Friction lining, Taguchi

## Introduction

Brake pads and linings are part of the disc brakes used in motor cars [1]. They are used in braking systems to control the vehicle's speed by converting the vehicle's kinetic energy to thermal energy through friction and releasing the heat generated into the environment. Drum brake and disc brake linings are the two types of brake linings used in automotive braking systems. The drum brake is housed inside a drum, and when the brakes are applied, the brake lining is pulled outward and pressed against the drum, whereas disc brakes work comparably but are unprotected [1–5]. The asbestos matrix is a component of the disc brakes, which are made up of a variety of materials [6]. Asbestos, which is a major constituent in brake lining production, is not readily available and is expensive. Asbestos is linked with the disease asbestosis, which is life-threatening [3]. Because of its carcinogenic and destructive characteristics, asbestos is being avoided in both developed and developing countries [1, 3, 4, 7, 8].

With the ongoing research on alternative materials for friction lining, the use of copper in friction lining is also reduced, which results in a meaningful change in the composition of friction materials in 2020 (a reduction of 0.5%). Due to the wear debris from friction materials that are washed into rivers when braking and contain copper, rules have been introduced in California and Washington to reduce this. The copper in this detritus is harmful to molluscs and prevents salmon from spawning. Therefore, copper-free brake friction materials have advanced, and there are also a few research articles and patents related to it [4].

The braking system was designed to assist in the gradual slowing down or complete stoppage of a moving vehicle [5, 9–11]. When the vehicle brake is applied, it is driven outwards and against the drum. Friction occurs between the revolving disc and the pad when the brake is applied. The brake pads must absorb heat fast, withstand high temperatures and not wear. When the brake is heated up by making contact with a drum or rotor, it begins to transfer a small quantity of friction material to the disc or lining [12]. This is why a brake disc is a dull grey [1, 3, 10, 13, 14]. Friction linings contain over ten ingredients mixed properly to achieve the expected combination of performance properties [3, 7, 15]. Aside from managing friction and wear resistance, friction linings are divided into four categories: binder, fibres, friction modifiers and fillers. In friction materials, a binder is a critical component that tightly binds the ingredients so they can perform the desired function [16]. Friction modifiers are used to adjust the required range of friction, whereas amalgamated fibres are frequently incorporated for strength. Functional fillers are used to improve particular characteristics of composites, such as fade resistance, and space/non-reactive fillers are used to save money [17, 18].

Due to in situ deterioration that begins at room temperature, these resins are heat- and humidity-sensitive, with a short shelf life. The features that make brake pads suitable for usage are assessed. Properties to be studied include abrasion resistance, hardness, friction coefficient, compressive strength, specific gravity, water and oil soaks, tensile strength, thermal conductivity, disc temperature and stopping time [3, 19].

The compositional design of friction materials is well-known to be difficult with multiple criteria optimization that involves not only the problems of handling different categories of ingredients but also reaching an expected level of performance [20]. The use of coconut shell (CS) and palm kernel shell (PKS) has been developed for asbestos-free brake pad materials [3, 6, 14]. Agro-industrial wastes are being studied as a source of raw materials in the industry all over the world. This method of disposal will not only be cost-effective, but it may also result in foreign exchange gains and environmental protection. After the phase-out of asbestos, which had received global recognition as a carcinogen, new materials and elements are now utilized in vehicle brake friction material, even though the asbestos prohibition in some countries was only implemented in 1989.

According to the previous study by Adeyemi et al. [21], palm kernel shells (PKS) can be used to fabricate brake pads and friction lining material since they showed good potential in the evaluation. PKS is both affordable and readily available. It has an impact on polymer composite manufacturing adhesion and dispersion.

Coconut shell brake pads were developed by Egeonu et al. [22]. Ground coconut shells (filler), epoxy resin (binder–matrix), iron chips (reinforcement), methyl ethyl ketone peroxide (catalyst), cobalt naphthenate (accelerator), iron and silica (abrasives)

and brass were added in the composition (friction modifier). The pulverized filler was sieved using a sieve with a 710- $\mu$ m aperture.

Breaking strength, hardness, compressive strength and impact all decreased as the proportion of ground coconut powder increased, showing that a high percentage of ground coconut powder causes brittleness [23].

Elakhame et al. [22] used periwinkle shells to produce brake pads. Periwinkle shell asbestos-free brake pad shape and characteristics were investigated. Crushed, powdered and sieved sun-dried periwinkle shells have sieve sizes of + 710, + 500, + 355, + 250 and + 125  $\mu$ m. The recipe called for periwinkle shell powder, phenolic resin (phenol-formaldehyde), motor oil (SEA 20/50), and water.

Idris et al. [6] studied and manufactured brake pads utilizing a binder made from peels of banana instead of asbestos. In a 5-wt. per cent interval, the resin was changed from 5 to 30% wt. Physical, mechanical, wear and morphological aspects of the brake pad have all been investigated. The results revealed that increasing the weight per cent of resin added increased compressive strength, hardness and specific gravity of the samples. The resin concentration grew as the oil soak, water soak, wear rate and % burned reduced. All the qualities were improved in the samples containing 25% uncarbonized banana peels (UNCBp) and 30% carbonized banana peels (CBp).

Sathyamoorthy et al. [11] in their review paper focused on providing in-depth details regarding the frequently used chemicals, manufacturing processes and properties of brake friction compounds.

Sathyamoorthy et al. [24] in another study, examined the impact of several abrasives (red mud, steel slag and fly ash) on the tribological properties of non-asbestos brake friction materials. By altering the ratios of crucial elements including red mud, steel slag, and fly ash while keeping the ratios of other basic ingredients, three different brake friction composites were created. As a result, friction composites made with various abrasives were created, and their mechanical, chemical and physical characteristics were assessed in accordance with industry requirements. The tribological characteristics were determined experimentally in accordance with IS2742 part 4 using the Chase friction test equipment. According to the experimental findings, fly ash particles in friction composites demonstrated consistent fade and recovery behaviours with a lower wear rate. In contrast, the recovery behaviour of steel slag-based friction composites was better.

In another study, iron sulphide is used as a solid lubricant with red mud as an abrasive to create brake friction composites utilizing traditional production methods in the shape of ordinary brake pads. By changing important ingredients like red mud and iron sulphide while maintaining the same levels of the other parental ingredients, three distinct brake friction composites were created. According to industry norms, experiments on the generated composites' physical, chemical, mechanical and thermal properties were conducted. Using a Chase friction test rig, the tribological performance was experimentally examined in accordance with IS2742 part 4. The experimental effort led to the conclusion that red mud and iron sulphide particles combined produced friction composites with stable fade and recovery behaviours. Conversely, the friction composites based on iron sulphide showed reduced wear. The surface properties of the friction composites evaluated by Chase were revealed by scanning electron microscopy (SEM) [25].

Akncioğlu et al. [26] reported in their study that 3.5% hazelnut shell dust was used as a natural additive material to create an eco-friendly brake composite sample. The Chase-type test machine and a newly created device were used to conduct friction testing on the manufactured pad sample and a commercial pad. The evaluation of the two distinct test device outcomes is given using a separate strategy. The braking performance of the sample with hazelnut shell dust was found to be in conformity with international standards after the trial results were compared using the Taguchi method. The findings from their study led to the nominal friction coefficient value being determined to be 0.505. The shearing forces of the eco-friendly brake composite pad and commercial pad samples were measured to be 607.3 and 850.5 N, respectively.

Another study investigated how brake pads made with walnut shell powder as a natural additive material affected braking performance. Two distinct kinds of samples of brake pads were made with 3.5 and 7% (2A and 2B) of walnut shell dust in the mix. As a benchmark, a commercial Clio brake tip was employed. The developed brake pads underwent microstructure analysis, testing for thermal conductivity, friction wear, density and hardness. Wear friction tests were conducted using a Chase-type equipment, and results were obtained in accordance with SAE-J661 (Brake Lining Quality Test Procedure) guidelines. The performances of the natural additive brake pads were assessed by comparing the experimental data to those of the commercial brake pads. Walnuts have been added [27].

Edokpia et al. [28] created and assessed eggshell (EG)-based eco-friendly (biodegradable) brake cushions. Gum Arabic (GA) was utilized as a folio. Both added substances were explored as a conceivable substitution for asbestos and formaldehyde gum which are carcinogenic in nature and non-biodegradable. The brake lining formulation was delivered by changing the GA from 3 to 18 wt %. Tests carried out on tests included wear rate, thickness swelling in water and SAE oil, warm resistance, particular gravity, compressive quality, hardness values and microstructure. Comes about appeared that definitions containing 15 to 18 wt % of GA created great holding. The test with 18 wt % of GA in ES particles gave the most excellent properties. Maize husk (MH)-based composite brake pads were developed by Adeyemi et al. [7]. The filler particulate size in their research was 300 microns, and the binder was epoxy resin. The study showed that decreasing the filler content increases the developed brake pad's hardness, wear rate, tensile strength, compressive strength and thermal conductivity, while increasing the filler content weight per cent enhances density, coefficient of friction, water absorption and oil absorption. The findings suggested that MH particles could be used to replace asbestos in the manufacturing of brake pads for automobiles. The new composite brake pad, unlike asbestos-based brake pads, is environmentally friendly and has no recognized health risks [15]. In their study, the physical, mechanical and tribological properties of the newly developed automotive brake pad were investigated. The results for the agro waste-based brake pads were superior to those of commercial brake pads and other existing brake pads.

Research has shown that agro wastes are potential materials for the development of friction linings [3, 7, 19, 22]. This work would improve on the existing PKS-based friction linings by mixing them with pulverized coconut shells, brass filings, iron filings, calcium carbonate and burnt vehicle tyres. PKS is economical and is available in abundance. It

has the characteristics of influencing the adhesion and dispersion of polymer composite fabrication. The physical and chemical characteristics of palm kernel shells were investigated [3, 21].

## Methods

### Materials

The materials used in this work are as follows: calabash (*Crescentia cujete*), palm kernel shell (*Elaeis guineensis*), burnt vehicle tyre powder (*used as carbon black*), iron fillings, brass fillings, aluminium fillings, phenol formaldehyde, alkyd resin, cashew nut shell liquid (CNSL), accelerator (rubber solution), catalyst (*DMP 30, 2,4,6-tri dimethylamino methyl phenol*), trisphenol hardener and calcium carbonate.

### Method

The method used in the production of the friction lining material was previously reported [3]. The friction lining material was synthesized by blending 50 ml of phenol-formaldehyde with 40 ml of alkyd resin; 10 mL CNSL was added to the uniformly blended mix, along with 4 g of charred tyres, and the mixture was thoroughly mixed. Twenty-five grams of palm kernel shell, 6 g of brass fillings, 4 g of aluminium fillings, and 5 g of iron filings were blended into the mixture. Slowly, 4 g of calabash and 6 g of calcium carbonate were added.

On obtaining a uniform blend, 5 ml of rubber solution and 3 ml of trisphenol hardener were added. The above ratio of phenolic resin and alkyd resin gave a pot life of 10–20 min. The mixture was thoroughly blended and transferred to a mould for compaction. The mixture was allowed to harden partly; it was subjected to a hydraulic press for compaction at a pressure of about 200 psi to give the shape of the mould.

The compacted sample was then subjected to a preliminary curing process of 60 °C for 2 h after which it was post-cured at 180 °C for 3 h in an oven.

### Experiment design

The Taguchi L9 orthogonal array was utilized to decide the ideal settings to produce the low wear friction lining by utilizing the signal-to-noise ratio (S/N) and the ANOVA.

### Material characterization

The samples were subjected to the following characterization: X-ray fluorescence spectroscopy (XRF), Fourier transform infrared spectroscopy (FTIR) and scanning electron microscopy energy dispersive spectroscopy (SEM-EDX).

#### XRF

The friction lining material sample was pulverized in a small container, and the elemental composition of the friction lining material was determined by placing the XRF spectrometer directly on the powdered sample.

#### FTIR

The FTIR spectra of the friction lining material were obtained from the Fourier transform infrared spectrometer (CARY 630, Agilent Technologies, USA) by mixing

thoroughly and pelletizing about 10 mg of the friction lining material (brake linings) with finely ground KBr to obtain a transparent disc and by placing the pelletized samples on the IR path. Wave numbers from 3800 to 600  $\text{cm}^{-1}$  were considered for the friction linings.

### SEM-EDX

The morphology of the friction lining material was observed from the Phenom ProX (Phenom World, Eindhoven, The Netherlands) SEM with an acceleration voltage of 10 kV and FOV of 537  $\mu\text{m}$ . The surfaces of the samples to be examined were made conductive by palladium-gold sputtering.

### Tribological tests

#### Wear rate

The wear rate was conducted using the pin-on-disc tribometer in accordance with ASTM G99. The pin-on-disc set-up is schematically represented in Fig. 1. The samples were clamped against the rotating disc of a dynamometer running at varying speeds on the application of braking pressure. The thickness was measured and weighed before and after the test to obtain the wear rate using Eq. (1).

$$\text{Wear rate, } \Delta w = \frac{W_2 - W_1}{S} \quad (1)$$

The sliding distance,  $S = 2\pi D N t / 6000$

where  $W_1$  is the weight before the test,  $W_2$  is the weight after the test,  $S$  is the sliding distance,  $D$  is the disc diameter,  $N$  is the radial speed (rpm) and  $t$  is the time taken to expose the specimen to wear.

### Results and discussion

#### Taguchi method

The friction lining material will be designed with a low wear rate in view. In the Taguchi design, the wear rate is the response. Table 1 depicts the experimental layout,

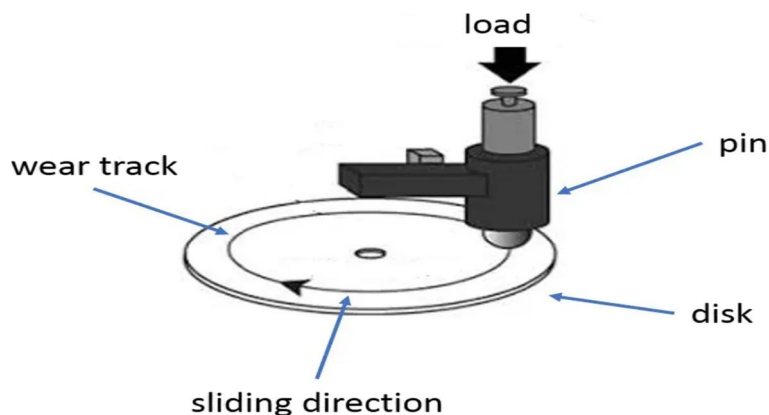


**Fig. 1** Schematic representation of wear test set-up

**Table 1** Experiment settings showing the factors and levels

Number	Parameters	Units	Levels		
1	A: Moulding temperature	°C	120	150	180
2	B: Curing time	min	10	15	20
3	C: Heat treatment time	h	2	4	10

which includes factors and levels. The experimental design matrix for wear rate with the S/N ratio and the means is shown in Table 2. Table 3 shows the S/N ratio response table.

The signal-to-noise ratio employed for the wear rate is the smaller-the-better, which is expressed mathematically as:

Smaller-the-better

$$\frac{S}{N} = -10\log_{10}y^2 \tag{2}$$

The delta represents the difference in response between the top and bottom. The robustness of the parameter on the response factor is shown by a large delta value, while the least effect on the response factor is shown by a low delta value. Tables 3 and 4 show that the most critical elements influencing friction lining wear rate are as follows: *heat treatment > moulding temperature > curing time*.

Figure 2 shows the main effects plots for means of wear rate while Fig. 3 shows the main effects plots for the signal-to-noise ratio of wear rate.

**Table 2** Experimental outlay for the wear rate

Experiment number	A: Moulding temperature	B: Curing time	C: Heat treatment time	Wear rate	S/N ratio	Means
1	1	1	1	0.740	2.6154	0.740
2	1	2	2	0.106	19.4939	0.106
3	1	3	3	0.107	19.4123	0.107
4	2	1	2	0.104	19.6593	0.104
5	2	2	3	0.100	20.0000	0.100
6	2	3	1	0.110	19.1721	0.110
7	3	1	3	0.103	19.7433	0.103
8	3	2	1	0.108	19.3315	0.108
9	3	3	2	0.400	2.6154	0.400

**Table 3** Response table for signal-to-noise ratios. Smaller-is-better

Level	A	B	C
1	13.84	14.01	13.71
2	19.61	19.61	15.70
3	15.68	15.51	19.72
Delta	5.77	5.60	6.01
Rank	2	3	1



**Table 4** Response table for the means

Level	A	B	C
1	0.3177	0.3157	0.3193
2	0.1047	0.1047	0.2033
3	0.2037	0.2057	0.1033
Delta	0.2130	0.2110	0.2160
Rank	2	3	1

A, B and C represents moulding temperature, curing time and heat treatment time, respectively

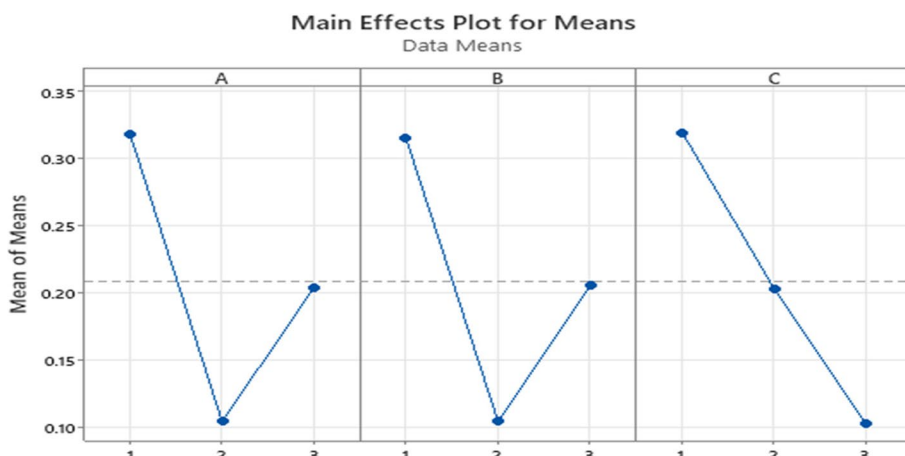
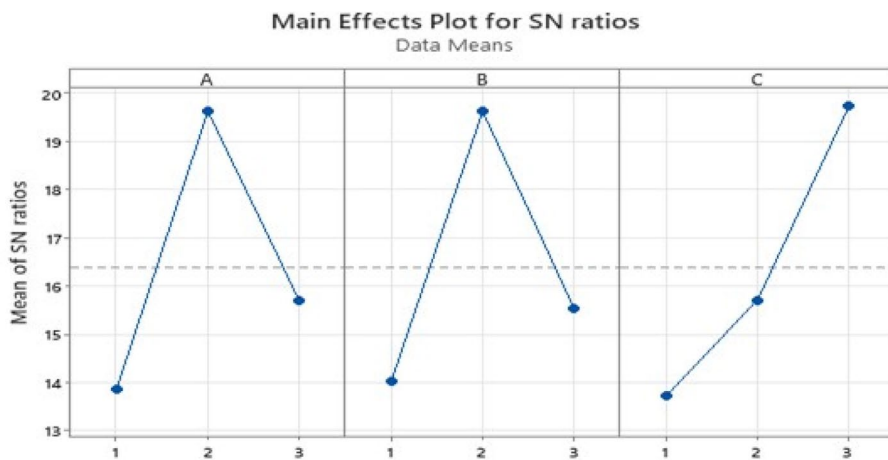


**Fig. 2** Main effects plots for the means of wear rate



Signal-to-noise: Smaller is better

**Fig. 3** Main effects plots for the signal-to-noise ratio of wear rate

**Analysis of variance (ANOVA)**

The ANOVA was used to investigate the variables that have a substantial impact on wear rates. The significance level can be determined by the percentage contribution, *P*. The *F*-test is a statistical method for identifying parameters that have a substantial



impact on quality features. The most significant factor is indicated by a lower  $P$ -value. The one-way ANOVA findings for wear rate are presented in Tables 5, 6 and 7. Heat treatment, as shown in Table 7, is the most significant factor affecting wear rate. The ANOVA result agrees with the results shown in Tables 3 and 4.

The  $F$  statistics ( $F$ -value) is combined with the  $P$ -value to ascertain if the ANOVA results are significant enough to reject the null hypothesis. This means that large values of the  $F$  statistics show that something is significant, while a small  $P$ -value shows that the results are significant. Table 7 has an alpha level of 0.05, with the highest  $F$ -value of 0.65 and the lowest  $P$ -value of 0.555. This means that heat treatment is the most important step in producing a low-wear friction lining material.

### Validation of experiments

The Taguchi design ends with the validation of experiments. The best circumstances for the selected relevant parameters are determined at this stage, and a specified number of experiments are carried out at the specified conditions. There is no requirement for a confirmatory test if the ideal combination of parameters and their values corresponds with any of the orthogonal array's experiments. Table 8 shows the optimum control factor settings, with A (2), B (2), and C (3) as the best combinations of parameters and levels (3).

**Table 5** One-way analysis of variance for the moulding temperature

Source	DF	Adj SS	Adj MS	F-value	P-value
A: Moulding temperature	2	0.06817	0.03408	0.63	0.565
Error	6	0.32543	0.05424		
Total	8	0.39360			
<b>S</b>	<b>R-sq</b>	<b>R-sq (adj)</b>	<b>R-sq (pred)</b>		
0.232892	17.32%	0.00%	0.00%		

**Table 6** One-way analysis of variance for the curing time

Source	DF	Adj SS	Adj MS	F-value	P-value
B: Curing time	2	0.06682	0.03341	0.61	0.572
Error	6	0.32678	0.05446		
Total	8	0.39360			
<b>S</b>	<b>R-sq</b>	<b>R-sq (adj)</b>	<b>R-sq (pred)</b>		
0.233372	16.98%	0.00%	0.00%		

**Table 7** One-way ANOVA results for the heat treatment

Source	DF	Adj SS	Adj MS	F-value	P-value
C: Heat treatment time	2	0.07011	0.03506	0.65	0.555
Error	6	0.32349	0.05391		
Total	8	0.39360			
<b>S</b>	<b>R-sq</b>	<b>R-sq (adj)</b>	<b>R-sq (pred)</b>		
0.232195	17.81%	0.00%	0.00%		

**Table 8** Optimal settings for control factors

Response	Control factor	Optimum settings
Wear rate	A: Moulding temperature	150
	B: Curing time	15
	C: Heat treatment	10

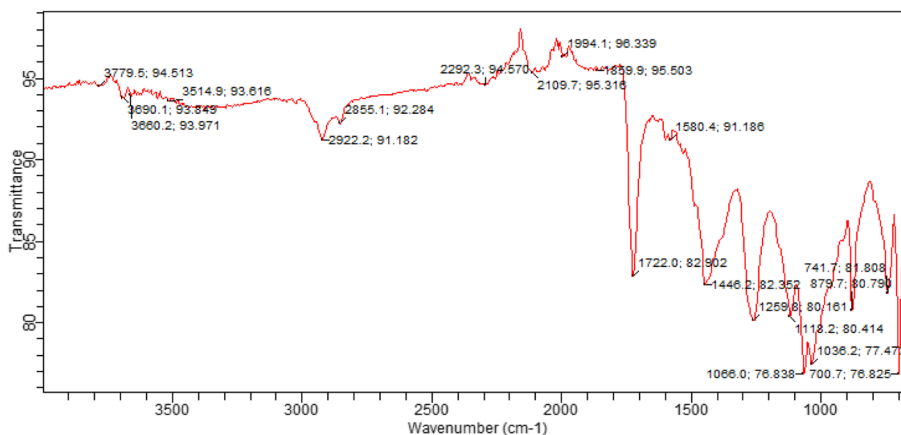


**Fig. 4** IR spectrum of the friction lining material developed

### Characterization of the friction lining materials

The friction lining characterized was produced using the optimum settings of the control factors which are A (2), B (2) and C (3) to produce a friction lining that has a low rate of wear.

### The fourier transform infrared (FTIR) spectroscopy studies for the friction lining materials

Figure 4 shows the FTIR spectrum of the friction lining material. Table 9 summarizes the entire absorption band assignment of the spectra. The spectra reveal a band at 3660  $\text{cm}^{-1}$  and 3690  $\text{cm}^{-1}$ , which correspond to inner hydroxyls and outer surface hydroxyl vibrations, respectively [29, 30]. There are bands between 2855 and 2922  $\text{cm}^{-1}$  in the sample, indicating that there are asymmetrical and symmetrical stretching vibrations of  $\text{CH}_2$  in an aliphatic hydrocarbon. Intense peaks attributable to  $\text{C}=\text{O}$  and  $\text{C}-\text{O}$  stretching vibrations of the  $\text{COOH}$  groups may be seen in the bands 1722  $\text{cm}^{-1}$ , 1580  $\text{cm}^{-1}$  and 1446  $\text{cm}^{-1}$ . The absorption bands of the stretching vibrations of triple bonds  $\text{C}\equiv\text{C}$  and  $\text{C}\equiv\text{N}$  are 2109  $\text{cm}^{-1}$ .

### X-ray fluorescence (XRF) spectroscopy results for the friction lining material

The XRF spectroscopy results conducted on the samples indicated that the developed friction lining materials contained the following compounds in large proportions with the counts:  $\text{CaO}$ , 43.593;  $\text{SiO}_2$ , 13.811;  $\text{Al}_2\text{O}_3$ , 11.977; and  $\text{Fe}_2\text{O}_3$ , 11.068. The following elements with the counts were found in large proportions: Ca, 6457.429; Fe, 3973; Zn, 679.499; Cu, 656.149; Pb, 544.101; Cl, 485.885; Ba, 291.655; and Si, 106.805.

**Table 9** Absorption bands in the FTIR spectra of friction lining material position and assignment

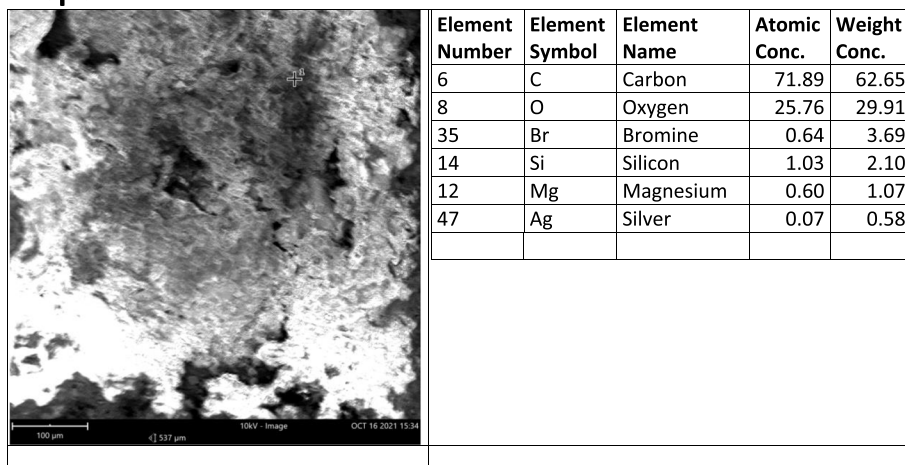
Assignment	Friction lining material (cm <sup>-1</sup> )
OH stretching of the inner surface hydroxyl groups ( <i>in plane vibration with a transition moment nearly perpendicular to the (001) plane</i> )	3690
OH stretching of the inner surface hydroxyl groups ( <i>anti-phase vibration with a transition moment lying in the (001) plane</i> )	3660
CH <sub>2</sub> stretching vibration ( <i>asymmetrical and symmetrical vibration of CH<sub>2</sub> in an aliphatic hydrocarbon</i> )	2922–2855
Intense peaks of C=O and C-O stretching vibrations of COOH groups ( <i>indicating the presence of modification</i> )	1722–1446
In-plane Si-O stretching	1036
Si-O, <i>perpendicular</i>	741

**Scanning electron microscopy-energy dispersive (SEM-EDX) spectroscopy results for the friction lining material**

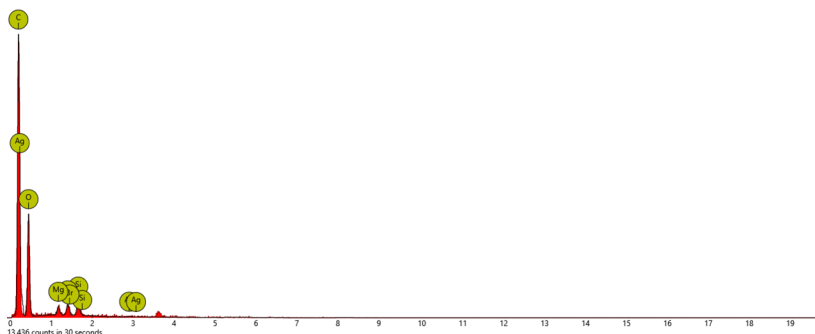
The image scans for two spots are presented in Figs. 5 and 6 and Tables 10 and 11 respectively at an acceleration voltage of 10 KV and FOV of 537 μm.

The SEM-EDX results for the two image scans show that carbon and oxygen were the most abundant elements, as seen in the micrograph and Tables 10 and 11. The

**1. spot**



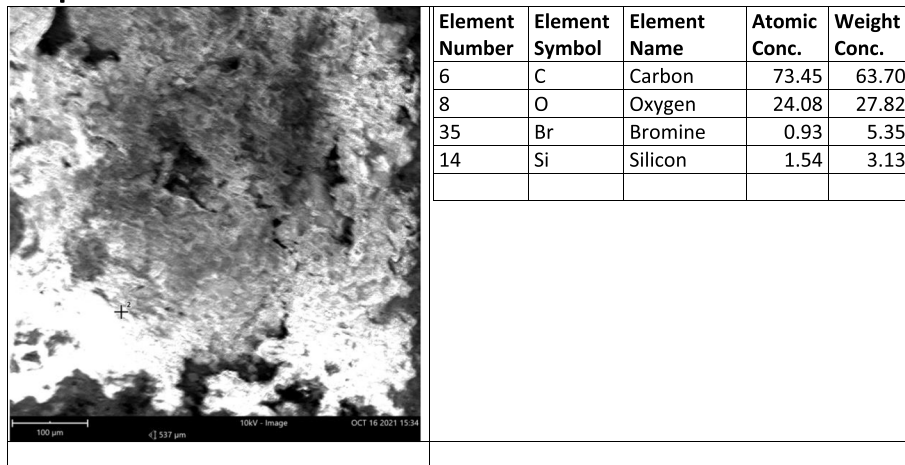
FOV: 537 μm, Mode: 10kV - Image, Detector: BSD Full, Time: OCT 16 2021 15:34



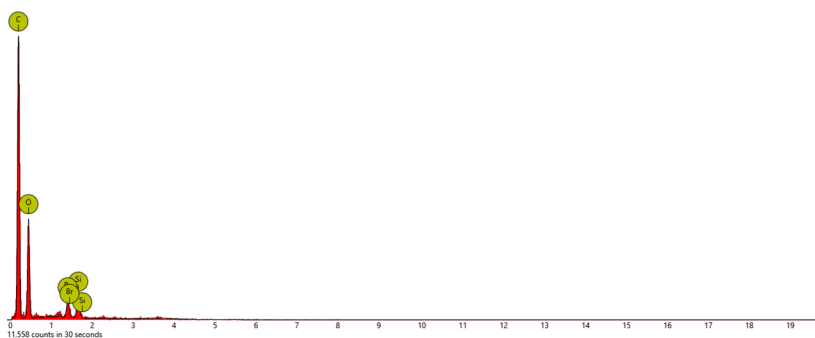
Disabled elements: B

**Fig. 5** Image 1 SEM-EDX for the friction lining material (FOV, 537 μm; mode, 10 kV—image, detector: BSD full, time October 16, 2021, 15:34)

## 2. spot



FOV: 537 μm, Mode: 10kV - Image, Detector: BSD Full, Time: OCT 16 2021 15:34



Disabled elements: B

**Fig. 6** Image 2 SEM-EDX for the friction lining material (FOV, 537 μm; mode, 10 kV—image, detector: BSD full, time October 16, 2021, 15:34)

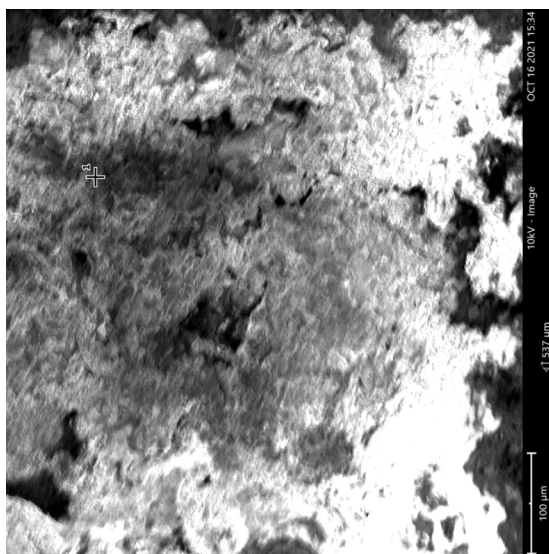
first image scanned showed carbon with an atomic concentration of 71.89 and a weight concentration of 62.65, while Fig. 5 depicts oxygen with an atomic concentration of 25.76 and a weight concentration of 29.91.

The second image scanned has a weight concentration of 63.70 and an atomic concentration of 73.45 for carbon, while Fig. 6 has a weight concentration of 27.82 and an atomic concentration of 24.08 for oxygen.

## Conclusions

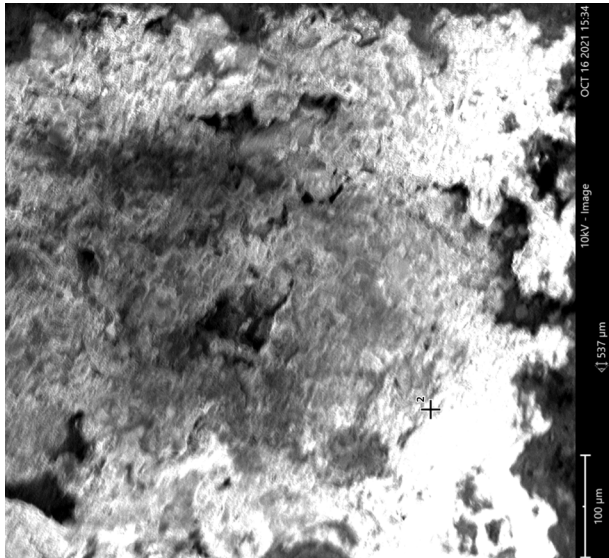
In this study, friction lining materials for motorcycles and tricycles were produced using machine shop scraps including brass and iron fillings, burnt tyre ash, coconut shell and palm kernel shell. Figure 7 is a sample of the friction lining material developed in this study. The Taguchi design method in the Minitab software was used to determine the optimal parameters necessary to produce friction lining materials with low wear rate. The final friction lining material was produced using the optimum combination of parameter settings and put through a series of material characterization tests. The optimum parameter settings from the Taguchi method were obtained

**Table 10** SEM-EDX morphology and results for the first image scan



Element Number	Element Symbol	Element Name	Atomic Conc.	Weight Conc.
6	C	Carbon	71.89	62.65
8	O	Oxygen	25.76	29.91
35	Br	Bromine	0.64	3.69
14	Si	Silicon	1.03	2.10
12	Mg	Magnesium	0.60	1.07
47	Ag	Silver	0.07	0.58

**Table 11** SEM-EDX morphology and results for the second image scan



Element Number	Element Symbol	Element Name	Atomic Conc.	Weight Conc.
6	C	Carbon	73.45	63.70
8	O	Oxygen	24.08	27.82
35	Br	Bromine	0.93	5.35
14	Si	Silicon	1.54	3.13



**Fig. 7** Sample of the friction lining material developed

for a low wear rate as follows: moulding temperature of 175 °C, cure time of 8 min and heat treatment of 3 h.

For the purpose of identifying the compounds and functional groups present, as well as the elemental composition and morphology of the developed friction lining materials, the friction lining material was subjected to X-ray fluorescence spectroscopy (XRF), Fourier transfer infrared spectroscopy (FTIR) and scanning electron microscopy-energy dispersive spectroscopy (SEM-EDX). According to the SEM-EDX findings, carbon and oxygen were the two main elements found in the micrograph. Carbon has an atomic concentration of 71.89 and a weight concentration of 62.65 in the first image that was scanned, while oxygen has an atomic concentration of 25.76 and a weight concentration of 29.91, as shown in Fig. 5. Carbon has an atomic concentration of 73.45 and a weight concentration of 63.70 in the second image that was scanned, while oxygen has an atomic concentration of 24.08 and a weight concentration of 27.82, as shown in Fig. 6. The friction lining material was subjected to XRF spectroscopy, and the results showed the following compounds in significant amounts by counts:  $\text{Al}_2\text{O}_3$ , 11.977;  $\text{SiO}_2$ , 13.811;  $\text{Fe}_2\text{O}_3$ , 11.068; and  $\text{CaO}$ , 43.593. Furthermore, the following elements with massive concentrations were found Ca is 6457.429, Fe is 3973, Zn is 679.499, Cu is 656.149, Pb is 544.101, Cl is 485.885, Ba is 291.655 and Si is 106.805. Table 9 provides a summary of the complete assignment of the absorption bands in the obtained IR spectra.



### Abbreviations

ANOVA	Analysis of variance
CBp	Carbonized banana peels
CNSL	Cashew nut shell liquid
CS	Coconut shell
EG	Eggshells
FTIR	Fourier transfer infrared spectroscopy
GA	Gum Arabic
MH	Maize husk
PKS	Palm kernel shell
SEM-EDX	Scanning electron microscopy-energy dispersive spectroscopy
XRF	X-ray fluorescence spectroscopy
S/N ratio	Signal-to-noise ratio
UNCBp	Uncarbonized banana peels

### Acknowledgements

The authors acknowledge the efforts of the management of the Federal University of Petroleum Resources in stimulating this research.

### Authors' contributions

All authors contributed to the study's conception and design. Material preparation, data collection and analysis were performed by COM, RUE, CEM and CMA. The first draft of the manuscript was written by COM, and all authors commented on the previous versions of the manuscript. All authors read and approved the final manuscript.

### Funding

The authors declare that no funds, grants or other support were received during the preparation of this manuscript.

### Availability of data and materials

The datasets used or analysed during the current study are available from the corresponding author on reasonable request.

### Declarations

#### Competing interests

The authors declare that they have no competing interests.

Received: 16 May 2022 Accepted: 30 July 2022

Published online: 29 August 2022

### References

1. Lawal SS, Bala KC, Alegbede AT (2017) Development and production of brake pad from sawdust composite. *Leonardo J. Sci* (30):47–56 Available: <http://repository.futminna.edu.ng:8080/xmlui/bitstream/handle/123456789/10375/DEVELO~1.PDF?sequence=1&isAllowed=y>
2. Surender SR (2017) Development of asbestos-free brake pads, pp 4449–4455 10.15680/IJRSET.2017.0603249
3. Mgbemena CO, Mgbemena CE, Okwu MO (2014) Thermal stability of pulverized palm kernel shell (PKS) based friction lining material locally developed from spent waste. *ChemXpress* 5(4):115–122
4. Vijay R, Lenin Singaravelu D, Filip P (2020) Influence of molybdenum disulfide particle size on friction and wear characteristics of non-asbestos-based copper-free brake friction composite. *Surf Rev Lett* 27(1). <https://doi.org/10.1142/S0218625X19500859>
5. Vijay R, Singaravelu DL, Jayaganthan R (2019) Development and characterization of stainless steel fiber-based copper-free brake liner formulation—a positive solution for steel fiber replacement. *Friction* 8(2):396–420. <https://doi.org/10.1007/s40544-019-0298-y>
6. Idris UD, Aigbodion VS, Abubakar IJ, Nwoye CI (2015) Eco-friendly asbestos free brake-pad: using banana peels. *J King Saud Univ Eng Sci* 27(2):185–192. <https://doi.org/10.1016/j.jksues.2013.06.006>
7. Ademoh NA, Adeyemi OI (2015) Development and evaluation of maize husks (asbestos-free) based brake pad. *Ind Eng Lett.* 5(2):67–80
8. Onyeneke FN, Aanae JU, Ugwuegbu CC (2014) Production of motor vehicle brake pad using local materials (periwinkle and coconut shell). *Int J Eng Sci* 3(9):17–24
9. Bhandari V (2011) Design of machine elements, third. Tata McGraw-Hill Education Private Limited, New Dehli
10. Rao RU, Babji G (2015) A review paper on alternate materials for asbestos brake pads and its characterization. *Int Res J Eng Technol.* 2(2):556–562
11. Sathyamoorthy G, Vijay R, Lenin Singaravelu D (2021) Brake friction composite materials: a review on classifications and influences of friction materials in braking performance with characterizations. *Proc Institution Mechan Engineers, Part J: J Eng Tribol*:1674–1706. <https://doi.org/10.1177/13506501211064082>
12. Yawas DS, Aku SY, Amaren SG (2016) Morphology and properties of periwinkle shell asbestos-free brake pad. *J King Saud Univ Eng Sci.* 28(1):103–109. <https://doi.org/10.1016/j.jksues.2013.11.002>
13. Bhandari V (2016) Design of machine elements, 3rd edn. Tata McGraw-Hill Education Private Limited
14. Owuama KC, Egbuna ICP, Nwaeto LO, Atah CM (2018) Asbestos free brake pad development using coal ash and palm kernel shell as filler material. *Equatorial J Eng*:59–70 Available: <https://www.academia.edu/38585162/ASBES>

TOS\_FREE\_BRAKE\_PAD\_DEVELOPMENT\_USING\_COAL\_ASH\_AND\_PALM\_KERNEL\_SHELL\_AS\_FILLER\_MATERIAL.

Accessed 19 Apr 2022.

15. Adeyemi O, Nuhu A, Boye T (2016) Development of asbestos-free automotive brake pad using ternary agro-waste fillers. *J Multidiscip Eng Sci Technol* 3(7):5307–323
16. Jubsilp C, Rimdusit S (2017) Polybenzoxazine-based self-lubricating and friction materials. *Adv Emerg Polybenzoxazine Sci Technol*:945–974. <https://doi.org/10.1016/B978-0-12-804170-3.00044-5>
17. Vasile C, Darie-Niță RN, Părpăriță E (2015) 10 – Performance of biomass filled polyolefin composites. In: *Biocomposites*, pp 257–301. <https://doi.org/10.1016/B978-1-78242-373-7.00012-3>
18. Elliot AJ (2015) Color and psychological functioning: a review of theoretical and empirical work. *Front Psychol*. 6:368. <https://doi.org/10.3389/FPSYG.2015.00368/BIBTEX>
19. Ibhadode AOA, Dagwa IM (2008) Development of asbestos-free friction lining material from palm kernel shell. *J Brazilian Soc Mech Sci Eng*. 30(2):166–173. <https://doi.org/10.1590/S1678-58782008000200010>
20. Ishola M, Oladimeji O, Paul K (2017) Development of ecofriendly automobile brake pad using different grade sizes of palm kernel shell powder. *Curr J Appl Sci Technol*. 23(2):1–14. <https://doi.org/10.9734/CJAST/2017/35766>
21. Adeyemi I, Ademoh N, Okwu M (2016) Development and assessment of composite brake pad using pulverized cocoa beans shells filler. *Int J Mater Sci Appl*. 5(2):66. <https://doi.org/10.11648/j.jijmsa.20160502.16>
22. Egeonu D, Oluah C, Okolo P (2015) Production of eco-friendly brake pad using raw materials sourced locally in Nsukka. *J Energy Technol Policy* 5(11):47–54 Available: [www.iiste.org](http://www.iiste.org). Accessed 01 May 2022
23. Irawan AP et al (2022) Overview of the important factors influencing the performance of eco-friendly brake pads. *Polym* 14(6):1180. <https://doi.org/10.3390/POLYM14061180>
24. Sathyamoorthy G, Vijay R, Singaravelu DL (2022) A comparative study on tribological characterisations of different abrasives based non-asbestos brake friction composites. *Mater Today Proc*. 56:661–668. <https://doi.org/10.1016/J.MATPR.2022.01.065>
25. Manoharan S, Sai Krishnan G, Ganesh Babu L, Vijay R, Lenin Singaravelu D (2019) Synergistic effect of red mud-iron sulfide particles on fade-recovery characteristics of non-asbestos organic brake friction composites. *Mater Res Express* 6(10). <https://doi.org/10.1088/2053-1591/AB366F>
26. Akıncioğlu G, Uygur İ, Akıncioğlu S, Öktem H (2021) Friction-wear performance in environmentally friendly brake composites: a comparison of two different test methods. *Polym Compos*. 42(9):4461–4477. <https://doi.org/10.1002/PC.26162>
27. Akıncioğlu G, Akıncioğlu S, Öktem H, Uygur İ (2020) Wear response of non-asbestos brake pad composites reinforced with walnut shell dust. *J Aust Ceram Soc* 56(3):1061–1072. <https://doi.org/10.1007/S41779-020-00452-6>
28. Edokpia RO, Aigbodion VS, Obiorah OB, Atuanya CU (2014) WITHDRAWN: evaluation of the properties of ecofriendly brake pad using egg shell particles–Gum Arabic. *Results Phys*. <https://doi.org/10.1016/j.rinp.2014.06.003>
29. Dai JC, Huang JT (1999) Surface modification of clays and clay–rubber composite. *Appl Clay Sci* 15(1–2):51–65. [https://doi.org/10.1016/S0169-1317\(99\)00020-4](https://doi.org/10.1016/S0169-1317(99)00020-4)
30. Huang CW et al (2012) Observation of strain effect on the suspended graphene by polarized Raman spectroscopy. *Nanoscale Res Lett* 7:1–6. <https://doi.org/10.1186/1556-276X-7-1>

## Publisher's Note

Springer Nature remains neutral with regard to jurisdictional claims in published maps and institutional affiliations.

Submit your manuscript to a SpringerOpen<sup>®</sup> journal and benefit from:

- Convenient online submission
- Rigorous peer review
- Open access: articles freely available online
- High visibility within the field
- Retaining the copyright to your article

---

Submit your next manuscript at ► [springeropen.com](https://www.springeropen.com)

---